Biochimica et Biophysica Acta, 766 (1984) 403–415
Elsevier

BBA 41563

NANOSECOND REDUCTION KINETICS OF PHOTOOXIDIZED CHLOROPHYLL-a_{II} (P-680) IN SINGLE FLASHES AS A PROBE FOR THE ELECTRON PATHWAY, H^+-RELEASE AND CHARGE ACCUMULATION IN THE O_2-EVOLVING COMPLEX *

K. BRETTEL, E. SCHLODDER and H.T. WITT

Max-Volmer-Institut für Biophysikalische und Physikalische Chemie, Technische Universität Berlin, Strasse des 17. Juni 135, D-1000 Berlin 12 (Germany)

(Received March 1st, 1984)

Key words: Chlorophyll a_{II}; Oxygen-evolving complex; S-state; Electron transfer; H^+ release; Photosynthesis

(1) The re-reduction kinetics of chlorophyll a_{II}^+ (P-680$^+$) after the first, second, third etc. flash given to dark-adapted subchloroplasts have been monitored at 824 nm in the nanosecond range. After the first flash and, again, after the fifth flash, the re-reduction of chlorophyll a_{II}^+ (Chl a_{II}^+) in the nanosecond range is nearly monophasic with $t_{1/2} \approx 23$ ns. After the second and third flash, the re-reduction is significantly slower and biphasic; it can be well-adapted with $t_{1/2} \approx 50$ ns and ≈ 260 ns. After the 4th flash, the re-reduction kinetics of Chl a_{II}^+ are intermediate between the first/fifth and second/third flash. A similar dependence on flash number was obtained with a sample of oxygen-evolving Photosystem II particles from *Synechococcus* sp. (2) Considering the populations of the S-states of the O_2-evolving complex before each flash, the following correlation of S-states to Chl a_{II}^+ reduction kinetics and electron transfer times, respectively, is obtained: in state S_0 as well as in state S_1 Chl a_{II}^+ is reduced with $t_{1/2} \approx 23$ ns, whereas in state S_2 as well as state S_3 a biphasic reduction with $t_{1/2} \approx 50$ ns and ≈ 260 ns (ratio of the amplitudes $\approx 1:1$) occurs. (3) The observed multiphasic Chl a_{II}^+ reduction under repetitive excitation is quantitatively explained by a superposition of the individual electron transfer times. (4) We suggest that the retardation of electron transfer to Chl a_{II}^+ in states S_2 and S_3 as compared to S_0 and S_1 is caused by Coulomb attraction by one positive charge located in the O_2-evolving complex. A positively charged O_2-evolving complex in states S_2 and S_3 can be explained if the electron release pattern (1,1,1,1) is accompanied by a proton release pattern (1,0,1,2) for the transitions ($S_0 \rightarrow S_1$, $S_1 \rightarrow S_2$, $S_2 \rightarrow S_3$, $S_3 \rightarrow S_0$). (5) A kinetic model based on linear electron transfer from the O_2-evolving complex (S) to Chl a_{II}^+ via two carriers, D_1 and D_2, makes a quantitative description of the experimental results possible. (6) According to the kinetic model, the retardation of electron transfer to Chl a_{II}^+ in states S_2 and S_3 is reflected by an increase in the change of standard free energy, ΔG^0, of the reaction Chl $a_{II}^+ D_1 D_2 S \underset{k_{-1}}{\overset{k_1}{\rightleftharpoons}}$ Chl $a_{II} D_1^+ D_2 S$ from $\Delta G^0 \approx -90$ meV in states S_0 and S_1 to $\Delta G^0 \approx -20$ meV in states S_2 and S_3. (7) This increase by ≈ 70 meV can be quantitatively explained by the Coulomb potential of the positive charge in the O_2-evolving complex, estimated by using the point charge approximation.

* This work has been presented in part at the 6th International Congress on Photosynthesis, Brussels (August 1983)

Abbreviations: ANT-2p, 2-(3-chloro-4-trifluoremethyl)anilino-3,5-dinitrothiophene; Chl, chlorophyll; Chl a_I, primary electron donor of Photosystem I; Chl a_{II}, primary electron donor of Photosystem II; D, electron carrier between the O_2-evolving complex and chlorophyll a_{II}^+; DMSO, dimethyl sulfoxide; FWHM, full width at half maximum; Mes, 4-morpholineethanesulphonic acid; Tricine, *N*-[2-hydroxy-1,1-bis(hydroxymethyl)ethyl]glycine; PQ, plastoquinone; PS, photosystem.

Introduction

The primary light reaction in Photosystem (PS) II leads to an electron transfer from the primary donor, Chl a_{II} (P-680) [1,2], to the first stable acceptor, PQ_1 (X-320) [3,4]. The photooxidized Chl a_{II} that ultimately oxidizes water to O_2 is directly re-reduced by an electron carrier, D, located between the O_2-evolving complex and Chl a_{II}. The redox reactions of Chl a_{II} are accompanied by absorption changes in the visible and near infrared [2,5,6]. Mainly the kinetics were investigated, following the characteristic bleaching of the Chl a_{II} absorption band at 680 nm [1,2] and the formation of a weak absorption of Chl a_{II}^+ at around 820 nm [5]. By a precise comparison of the kinetics at both wavelengths an identical behavior was found in oxygen-evolving PS II particles [7].

The re-reduction of Chl a_{II}^+ proceeds, for the most part, in the nanosecond range: it was measured at 820 nm that in dark-adapted samples, after one single turnover flash, the re-reduction is dominated by a 25–45 ns phase [8]. This is supported by measurements based on changes of fluorescence yield [9–11]. Under repetitive excitation, complex Chl a_{II}^+ reduction kinetics were observed which could be adapted by a multiphasic exponential decay. In the nanosecond time range, two phases ($t_{1/2} \approx 30$ ns ($\approx 50\%$) and $t_{1/2} \approx 250$ ns ($\approx 20\%$) [12]) or – under conditions of an improved signal to noise ratio – even three phases (20 ns (33%), 50 ns (19%) and 300 ns (19%) [7]) have been used in order to describe the reduction kinetics. The remaining approx. 30% decay with half-life times in the microsecond range.

Photosynthetic oxygen evolution requires the stepwise accumulation of four oxidizing equivalents in the O_2-evolving complex by four subsequent turnovers of Chl a_{II} in order to decompose 2 H_2O into 1 O_2 and 4 H^+. This conclusion is based on the observation that the yield of O_2 evolved by consecutive flashes given to a dark adapted sample shows an oscillation with a periodicity of four [13]. According to Kok [14] this is the case because the O_2-evolving complex passes through four different states (S_0, S_1, S_2, S_3) before oxygen is released during the transition $S_3 \rightarrow S_0$. The oscillation is damped due to inefficiencies in the process of accumulation of oxidizing equivalents ('misses') and double turnovers ('double hits') [15]. In dark adapted samples, usually 25% of the O_2-evolving complexes are in state S_0 and 75% in state S_1 [15]. Therefore, after the first flash, no O_2 is evolved and the first maximum in O_2 yield appears with the 3rd flash. Thus, after the first single turnover flash, the reduction of Chl a_{II}^+ is mainly related to the transition from S_1 to S_2. Under repetitive excitation, the four S-states are equally populated and equal amounts of O_2 are evolved after each flash. Correspondingly, all S-states are involved in electron donation to Chl a_{II}^+ under repetitive excitation. Comprehensive insights into the donor side of PS II should be obtained, if the Chl a_{II}^+ reduction is measured after the first, second, third, fourth, fifth, etc. flash, i.e., under conditions where the Chl a_{II}^+ reduction is selectively related to different S-state transitions.

The aim of the present study is to prove how the Chl-a_{II}^+ reduction kinetics – measured in a series of single flashes given to a dark-adapted sample – depend on the S-states of the O_2-evolving complex. For the carrier D between Chl-a_{II} and the O_2-evolving complex it was reported that its re-reduction by the O_2-evolving complex depends on the S-states [16]. A dependence of the Chl a_{II}^+ reduction kinetics on the S-states was proposed earlier based on measurements of delayed fluorescence [17], fluorescence yield [18], and absorption changes at 690 nm in the microsecond range [19]. In the present work, the Chl a_{II}^+ reduction was measured in the nanosecond range, monitoring absorption changes at 824 nm. An advantage of this method is that the measuring light is not absorbed by the sample, so that the S-state distribution remains undisturbed.

The determination of different Chl a_{II}^+ reduction kinetics related to the S-states may reveal the meaning of the multiphasic reduction under repetitive excitation, help to elucidate the four-step mechanism of photosynthetic oxygen evolution and offer a new possibility for monitoring the S-states.

Materials and Methods

Subchloroplasts from spinach were prepared by modification of the first steps of the procedure in Ref. 20: the broken chloroplasts were washed three times in 300 mM sucrose, 5 mM NaCl and 10 mM

Tricine buffer (pH 7.4) and finally suspended in 100 mM sucrose, 5 mM NaCl and 10 mM sodium phosphate buffer (pH 7.4). After two YEDA-press treatments at 10 MPa and removal of starch grains and unbroken lamellae by centrifugation ($1000 \times g$, 5 min), the membranes were suspended in 300 mM sucrose, 2.5 mM NaCl, 5 mM sodium phosphate buffer (pH 7.4) and 5% DMSO and stored in liquid nitrogen in the dark. Unless specified otherwise, the suspension used for the measurements contained: $1.8 \cdot 10^{-4}$ M Chl/$1 \cdot 10^{-3}$ M $K_3Fe(CN)_6$/30 mM sucrose/0.5 mM Na_2HPO_4/10 mM NaCl/2 mM $MgCl_2$/20 mM Tricine (pH 7.5)/0.5% DMSO. This preparation exhibits strongly reduced light scattering.

Oxygen-evolving PS-II particles from the thermophilic cyanobacterium *Synechococcus* sp. were prepared as described by Schatz and Witt [21] and stored at $-80\,^{\circ}C$ in the dark. They are enriched in PS II reaction centers (Chl: Chl $a_{II} \approx 90$; PS II: PS I > 20) and exhibit strongly reduced light scattering. The suspension used for the measurements contained: $5 \cdot 10^{-5}$ M Chl, 10^{-3} M $K_3Fe(CN)_6$, 10^{-2} M $MgCl_2$, 0.5 M mannitol and $2 \cdot 10^{-2}$ M Mes/NaOH (pH 6.5).

The time course of flash-induced absorption changes at 824 nm was measured using an equipment essentially described in Ref. 12. Excitation was performed by 3 ns (FWHM) laser flashes at 532 nm from a frequency doubled Nd/YAG laser (YG 441 from Quantel), yielding pulse energies up to 100 mJ. In flash series, the dark time between the flashes was 1 s. The measuring light source was a laser diode (CQL 12 from AEG) emitting 8 mW at 824 nm, spectral width approx. 5 nm (FWHM). Its light was focused by a microscope objective through a cuvette containing the sample (optical path length, 30 or 50 nm) and an interference filter onto a photodiode (FND 100 from EG&G or C 30952E from RCA). After appropriate amplification (amplifiers TVV 123 from Telemeter or 461a from Hewlett Packard), the signals were digitized by a Biomation 6500 transient recorder at a sampling interval of usually 2 ns and stored or accumulated by a Nicolet 1170 signal averager. The electrical bandwidth of the detection system was 100 Hz to 100 MHz with the FND 100 or 1 kHz to 50 MHz with the C30952E. Using the oxygen-evolving PS-II particles, a signal-to-noise ratio of approx. 5:1 is achieved without averaging (see Fig. 5); this is by one order of magnitude better than in previous measurements where more than 100 signals had to be averaged in order to obtain this signal-to-noise ratio [8,12]. All measurements were performed at room temperature in the dark. In order to assure dark adaptation of the samples at the beginning of the measurements, also thawing and diluting of the stock suspension were carried out in the dark, followed by a further dark time of at least 5 min. The measuring light at 824 nm does not disturb dark adaptation, since the unexcited sample does not absorb at this wavelength.

Measurement of absorption changes induced by each individual flash in a flash series given to dark-adapted subchloroplasts, was performed as follows: if the absorption change induced by the nth flash should be measured, $n-1$ oversaturating flashes were given to a new, dark-adapted sample followed by a flash that was attenuated by neutral density filters to an energy, corresponding to approx. 70% saturation. Only for this attenuated flash, the absorption changes were recorded. This procedure diminishes interference from components which contribute significantly only at oversaturating excitation [7], but assures full saturation by the preceding flashes.

In oxygen-evolving PS-II particles, due to quantitative limitation of the material, the absorption changes in a flash series were recorded using only one dark-adapted sample; this sample was illuminated by four subsequent saturating flashes of equal energy. The signals induced by these four flashes were stored in the four quarters of the memory of the Nicolet 1170.

Most signals were transmitted to an Apple II microcomputer and fitted by means of least-squares curve fitting programs (according to the program CURFIT in Ref. 22). The time at which the flash-induced absorption increase has reached half its maximum was taken as time zero. The next five data points (i.e., 10 ns) were not taken into account for the fit, since under our experimental conditions all signals contain a fast peak (half-life of decay, approx. 5 ns, corresponding to the instrumental response time) which is probably related to a process in the antennae system and not to Chl a_{II} (cf. Ref. 7). The following 800 data

points were fitted by either a monophasic, biphasic or triphasic exponential decay. Contributions from phases decaying in the microsecond and millisecond range were taken into account by addition of a slightly declining straight line. In the one- and two-exponential fit, both half-life times and amplitudes of the exponential phases and the initial amplitude of the straight line were taken as parameters. In the three-exponential fit, all half-life times were fixed and only the four amplitudes (including the initial amplitude of the straight line) were taken as parameters.

Results

Fig. 1 shows the time-course of the 824 nm absorption changes in subchloroplasts after each of five single turnover flashes given to a dark-adapted sample. The decay of the flash-induced absorption in the depicted time range is significantly slower after the second and third flash than after the first and fifth one. After the fourth flash, the decay is intermediate between the first/fifth and the second/third flash. This qualitative description is supported by the quantitative data evaluated by the one-exponential fit (see Table I).

The adaptation of the decay in the 10–1600 ns range by one exponential phase is quite good for the first flash and still acceptable for the fifth flash; for the second, third and fourth flash, however, at least two exponential phases are required for a good adaptation of the measured time course. For the third flash, for instance, this is illustrated in Fig. 2; the difference between recorded signal and fitting fucntion shows non-random deviations for the one-exponential fit (positive residuals in the range up to about 50 ns, negative ones in the 100–200 ns range and, again, slightly positive residuals from 300 to 800 ns), whereas the deviations are fairly random for the two-exponential fit. In Table I, besides the results of the one- and two-exponential fits, the ratios of the χ^2 values for both fits are also given, where χ^2 denotes the sum of the squares of deviations between data points and fitting function. The more this ratio exceeds the minimum value of 1, the worse gets the adaptation

TABLE I

RESULTS OF THE ONE- AND TWO-EXPONENTIAL FITS FOR THE SIGNALS IN FIGS. 1, 3 AND 4

$t_{1/2}$, half-life time; χ^2, sum of the squares of deviations between data points and fitting function. The fits are restricted to the decay in the range from 10 ns to 1.6 μs (cf. Materials and Methods), which is attributed to the reduction of Chl a_{II}^{+}.

Flash number or other conditions	One-exp. fit	Two-exp. fit		χ^2 (one-exp. fit)/ χ^2 (two-exp. fit)
	$t_{1/2}$ (ns)	$t_{1/2}$ (ns)	relative amplitude	
1	30	27	0.94	1.00
		1880	0.06	
2	133	47	0.58	1.13
		263	0.42	
3	131	48	0.63	1.18
		302	0.37	
4	92	30	0.73	1.13
		280	0.27	
5	36	21	0.86	1.05
		193	0.14	
repetitive excitation	96	23	0.68	1.78 [a]
		183	0.32	
+ANT-2p repetitive excitation	36	22	0.89	1.23 [a]
		209	0.11	

[a] These values cannot be compared directly to those in the upper part of the table because of the better signal-to-noise ratio in the measurements under repetitve excitation.

by the one-exponential fit compared to the two-exponential fit. The χ^2 ratios calculated for the fits to the first up to the 5th flash (Table 1) verify that for the second, third and fourth flash the one-exponential fit is considerably worse than the two-exponential fit. The fitting functions resulting from the two-exponential fits are depicted as solid lines in Fig. 1.

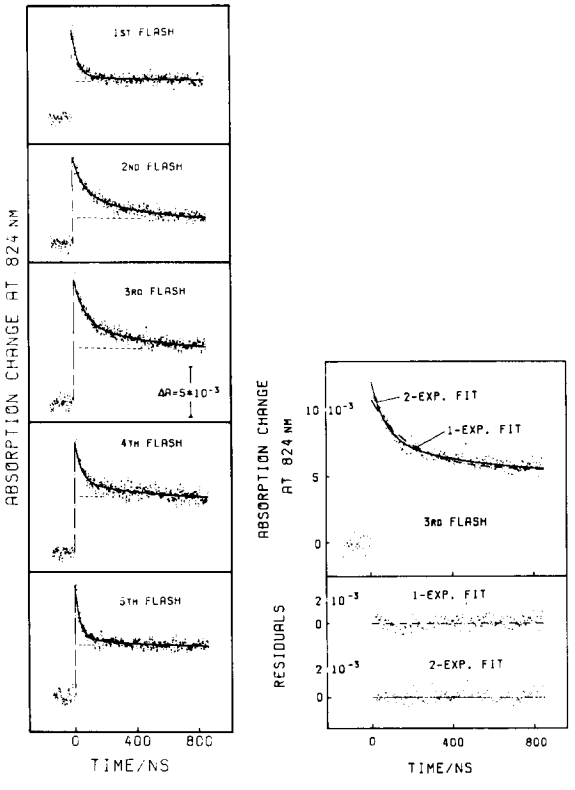

Fig. 1. Time-course of the absorption changes at 824 nm induced by each flash of a series of five laser flashes (≈ 3 ns FWHM, 532 nm) given to dark-adapted samples of subchloroplasts from spinach. The signal for the nth flash results from an approx. 70% saturating flash (approx. 0.3 mJ/cm^2), preceeded by $n-1$ oversaturating flashes (approx. 2 mJ/cm^2); the dark time between flashes was 1 s. Each signal is the average of eight measurements. Electrical bandwidth, 1 kHz–50 MHz. $1.8 \cdot 10^{-4}$ M Chl (pH 7.5)/1 mM $K_3Fe(CN)_6$ as electron acceptor; optical path, 50 mm. The solid lines represent the two-exponential fits (for data see Table I). The broken lines are the extrapolation of phases decaying in the microsecond and millisecond range.

Fig. 2. Top, comparison between one-exponential fit and two-exponential fit to the signal induced by the third flash in Fig. 1 (for data see Table I). Bottom, difference between recorded signal and fitting function; the residuals are plotted starting with the first point used for the fits, i.e., 12 ns after time zero.

The signals in Fig. 1 show significant variations also in the absorption level remaining at the end of the presented time range (850 ns). Measurements up to the millisecond range (not shown) revealed that these variations are mainly caused by a slowly (over 1 ms) decaying component. We attribute this slow decay to the re-reduction of Chl a_I^+ (or P-700$^+$), the photooxidized primary donor of PS I, which shows similar absorption around 824 nm as Chl a_{II}^+ [23]. This explanation is corroborated by the fact that no comparable variations of the amplitude of the slowly decaying absorption change was observed in PS-II particles (see Fig. 5) which contain less than one Chl a_I per 20 Chl a_{II} [21]. With respect to decay phases in the μs range (approx. 1/3) of the amplitude of the nanosecond phases in Fig. 1), more detailed investigations are in preparation.

The characteristic time courses depicted in Fig. 1 are not a special feature of very long dark-adapted samples: in samples which already had obtained a few flashes, followed by dark-adaptation for 20 min, again the significant variations of the absorption decay kinetics in a flash series were observed.

Fig. 3 shows the time course of the absorption changes at 824 nm in the presence of ANT-2p under repetitive excitation. The decay in the nanosecond range is nearly monophasic and similar to that observed after the first and fifth flash without ANT-2p (see Fig. 1 and the data for the 1- and 2-exponential fit in Table I). ANT-2p was added in this experiment in order to realize a high population of state S_1, even under repetitive excitation (see the first subsection under Discussion, p. 409).

Fig. 4 shows the time course under repetitive excitation under normal conditions (i.e., without ANT-2p). The kinetics are complex and intermediate between those observed in response to the first five flashes (see Fig. 1). The quantitative analysis of the signal (see Table I) reveals that at least two exponential phases are required for a good adaptation of the decay in the nanosecond range. The solid curve in Fig. 4 has been calculated as explained in the above-mentioned subsection (p. 409).

To generalize the results from spinach subchloroplasts, the 824 nm absorption changes induced

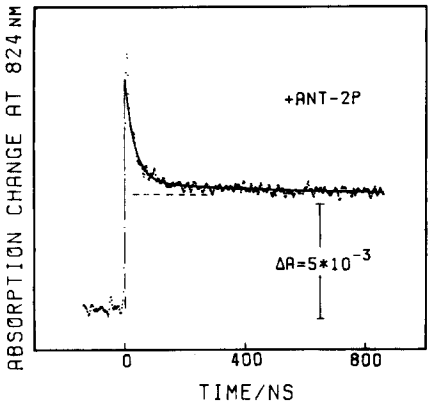

Fig. 3. Time-course of the flash-induced absorption change at 824 nm in subchloroplasts from spinach in the presence of 1 μM ANT-2p, under repetitive excitation; dark time between flashes, 1 s; excitation energy, approx. 0.3 mJ/cm^2; average of 64 sweeps; other details as in Fig. 1. The solid line represents the two-exponential fit (for data see Table I).

by consecutive flashes given after dark-adaptation, were also measured for oxygen-evolving PS II particles from *Synechococcus* sp. (Fig. 5). The observed dependence on flash number of the decay in the nanosecond range is very similar to that in subchloroplasts. Replacement of the electron acceptor $K_3Fe(CN)_6$ by phenyl-*p*-benzoquinone

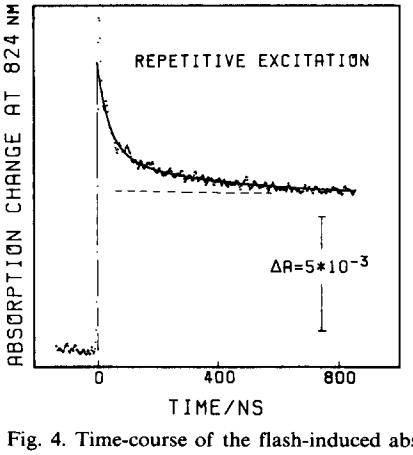

Fig. 4. Time-course of the flash-induced absorption change at 824 nm in subchloroplasts from spinach, under repetitive excitation; experimental conditions as in Fig. 3, but without ANT-2p. The solid line was calculated using three exponential phases with $t_{1/2}$ = 23 ns (50%), 50 ns (25%) and 260 ns (25%) (see the first subsection under Discussion), plus extrapolation of phases decaying in the microsecond and millisecond range (broken line).

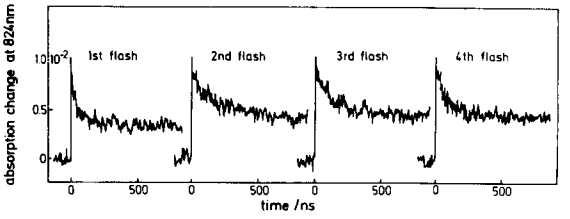

Fig. 5. Time-course of the absorption changes at 824 nm induced by each flash of a series of four saturating laser flashes (approx. 1.5 mJ/cm^2, 532 nm, 3 ns FWHM; dark time between flashes, 1 s) given to a dark-adapted sample of PS-II particles from *Synechococcus* sp.; each signal is the result of one measurement only (no averaging); $5 \cdot 10^{-5}$ M Chl (pH 6.5)/1 mM $K_3Fe(CN)_6$ as electron acceptor; optical path, 30 mm; electrical bandwidth, 100 Hz–100 MHz.)

(not shown) did not significantly alter the signals depicted in Fig. 5.

The absorption changes remaining at the end of the time scale presented in Fig. 5 decay, for the most part, in the microsecond range (not shown). Since the PS-II particles used in Fig. 5 contain only a negligible amount of PS I (PS II : PS I > 20), the microsecond phases can be attributed mainly to Chl a_{II}. Obvious variations of the total amplitude of the microsecond phases are not observed (see Fig. 5).

Discussion

In the present work absorption changes at 824 nm in a series of flashes given to a dark-adapted sample have been measured with nanosecond time resolution. Based on results from Refs. 7, 8 and 12 we attribute the 824 nm absorption changes, decaying with half-life times between approx. 20 ns and approx. 1 μs, to the re-reduction of Chl a_{II}^+ by electron transfer from water via secondary donors. The time-course of re-reduction was found to depend strongly on flash number in a series of single turnover flashes. The dependence is very similar in subchloroplasts from spinach and in oxygen-evolving PS-II particles prepared from cyanobacteria *Synechococcus* sp. (cf. Figs. 1 and 5), indicating a common feature of oxygen-evolving photosynthetic organisms.

A very fast absorption transient (half-life of decay not over approx. 5 ns) observed in the presented measurements is probably due to forma-

tion and decay of the triplet state and/or the lowest excited singlet state of Chl *a* [7]. This transient was omitted in the quantitative evaluation of the signals. Since the minor phases in the μs range (cf. Refs. 24–26 and 12) have not been investigated in detail in the present work, we restrict the following discussion to the rereduction of Chl a_{II}^+ with half-life times in the range from approx. 20 ns to approx. 1 μs.

Correlation of the different Chl a_{II}^+ reduction kinetics to the S-states of the O_2-evolving complex

An essential change taking place in PS II in a series of flashes is the change of the S-state, correlated to the change in the redox state of the O_2-evolving complex due to extraction of electrons by Chl a_{II}^+ and proton release. Different reactions at the donor side of PS II have been reported to depend on the S-states [14,27,16–19]. We suggest that also the different kinetics of Chl a_{II}^+ reduction in the nanosecond range are due to the different S-states. In order to prove whether this suggestion can account for our experimental results, we tried to correlate the measured decay kinetics with the S-states.

Fig. 6a–d shows the relative populations of states S_0 to S_3 prior to each flash as a function of flash number. These values have been calculated by assuming a probability $\alpha = 0.15$ for 'misses' and a dark distribution prior to the first flash of either $S_0 = 25\%$, $S_1 = 75\%$, $S_2 = S_3 = 0$ (squares) or $S_0 = 0\%$, $S_1 = 100\%$, $S_2 = 0$, $S_3 = 0$ (circles); 'double hits' were neglected. These parameters are based on literature data fitting oxygen-evolution patterns in flash series [27,28]. The different dark distributions were used since literature is controversial as to whether or not $K_3Fe(CN)_6$ oxidizes S_0 to S_1 in the dark [27,28]. Neglecting 'double hits' is justified by the short excitation pulse (3 ns) and by Jursinic's finding [28] that the probability of 'non-photochemical double hits' is only about 0.02 for freshly prepared chloroplasts, measured under excitation with laser flashes of 5 ns duration. This value drops below 0.01 by freezing and rethawing of the sample [28], as done in the present study.

A qualitative correlation between Chl a_{II}^+ decay and the S-states can be obtained by comparing the populations of the S-states (Fig. 6a–d) with the relative amplitudes of the different Chl a_{II}^+ reduction phases (Table I). After the first and after the fifth flash the reduction kinetics are dominated by a very fast phase ($t_{1/2} \approx 23$ ns, over 85%). In both cases the sum of population of S_0 and S_1 before the flash is approx. 100% (Fig. 6c), although the contributions of S_0 and S_1 are rather different for the first and the fifth flash, respectively (see Fig. 6a). Therefore, we tentatively correlate S_0 as well as S_1 with the very fast ($t_{1/2} \approx 23$ ns) reduction of Chl a_{II}^+. The correlation to S_1 is additionally supported by the very fast ($t_{1/2} \approx 23$ ns) Chl a_{II}^+ reduction in the presence of ANT-2p, under repetitive excitation (Fig. 3 and Table I). In this case, S_1 is predominantly present because ANT-2p accelerates the reduction of states S_2 and S_3 to S_1 [29].

After the second and the third flash, the Chl a_{II}^+ reduction is clearly slower than after the first and fifth flash (see Fig. 1 and Table I). Fig. 6b shows that prior to the second flash most O_2-evolving complexes are in state S_2 and that prior to the third flash mostly S_2 and S_3 are populated. Therefor, one can rougly correlate the slower kinetics to S_2 and S_3. This correlation becomes complicated by the fact that after the second and third flash the slower kinetics in the nanosecond range are significantly biphasic (see Table I and Fig. 2). It remains to be determined if the two phases are caused (α) by superposition of different S-states, each of which is related to a monophasic reduction of Chl a_{II}^+, or (β) if state S_2 as well as state S_3 are per se related to biphasic reduction kinetics of Chl a_{II}^+. Obviously, the latter assumption (β) would well explain the similar biphasic time-courses after the second flash ($S_2 \gtrsim 75\%$, $S_3 = 0$) and after the third flash ($S_2 + S_3 > 90\%$). In order to prove the former assumption (α), one might relate the slow phase (260 ns) to S_2 and the fast phase (50 ns) to S_3. This would be a good explanation for the bisphasic reduction kinetics after the third flash ($S_3 \approx 60\%$, $S_2 \approx 30\%$). However, the observed biphasic kinetics after the second flash (see Table I) differ significantly from a superposition of approx. 75% with 260 ns (due to S_2) and approx. 25% with 23 ns (due to S_1). This provides first evidence against the former assumption (α).

For a more general determination of the relationship between Chl a_{II}^+ reduction phases and

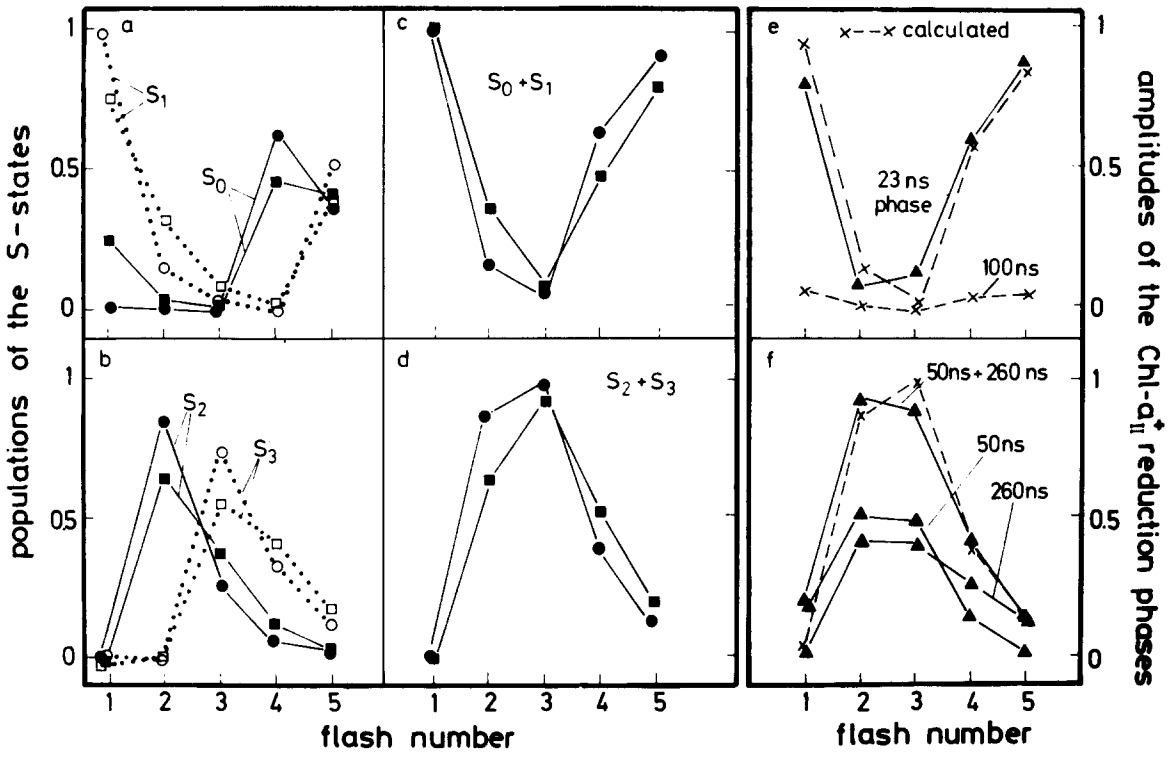

Fig. 6. (a–d) Relative populations of the S-states prior to each flash in a series of short (below approx. 3 ns) saturating flashes given after dark adaptation, plotted as a function of flash number. These populations were calculated assuming a probability $\alpha = 0.15$ for misses, no double hits, and a dark-distribution of either $S_0 = 0.25$, $S_1 = 0.75$, $S_2 = S_3 = 0$ (squares) or $S_0 = 0$, $S_1 = 1$, $S_2 = S_3 = 0$ (circles). (e,f) Amplitudes of the Chl a_{II}^{+} reduction phases as a function of flash number in a series of flashes given after dark adaptation: ▲———▲, obtained by three-exponential fits to the measured signals (Fig. 1) as described in the first subsection under Discussion. The amplitudes are normalized to the sum of the three phases. ×------×, calculated according to the kinetic model proposed in the next subsection. For details see text.

S-states we made the following comparison.

From the formal two-exponential fit and the foregoing discussion it becomes obvious that at least three different phases ($t_{1/2} \approx 23$ ns, ≈50 ns and ≈260 ns) contribute to the Chl a_{II}^{+} reduction in the nanosecond range.

To obtain a quantitative correlation between the amplitudes of the Chl a_{II}^{+} reduction phases and the S-states, the signals in Fig. 1 were fitted by three exponentials with fixed half-life times of 23, 50 and 260 ns. These values were taken as representative averages for the different half-life times evaluated from the two-exponential fits to the signals from the first, second, third and fifth flash and from the ANT-2p experiment (see Table I). The relative amplitudes resulting from the three-exponential fits are depicted in Figs. 6e and 6f (triangles, solid lines). From a comparison of the populations of the S-states (Fig. 6a–d), with the amplitudes of the three Chl a_{II}^{+} reduction phases (Fig. 6e and f), both as function of the flash number, we conclude:

the ≈23 ns phase is clearly correlated to S_0 and S_1, but neither to S_0 nor to S_1 exclusively (a slower phase related to S_0 and S_1 may contribute to the nanosecond decay with an amplitude of not over approx. 10%);

the ≈ 50 ns and the ≈260 ns phases are correlated to S_2 and S_3 but neither one to S_2 or S_3 exclusively. The ratio of the amplitudes of the two phases is approx. 1 : 1.

The evaluated correlation can be further examined by means of the kinetics observed under repetitive excitation (Fig. 4). In this case, the four

S-states are equally populated (i.e., 25% each). Therefore, according to the proposed correlation, the Chl a_{II}^+ reduction should be triphasic with 50% of a 23 ns phase (due to 25% S_0 and 25% S_1) and 50% of the two phases with 50 ns and 260 ns (due to 25% S_2 and 25% S_3).

The solid line in Fig. 4 is the result of such a superposition and corresponds very well to the signal measured under repetitive excitation. The same correspondence has been shown recently for the nanosecond kinetics measured with an improved signal-to-noise ratio in O_2-evolving PS II particles [7]. This demonstrates that the multiphasic decay under repetitive excitation can be explained on the basis of the results obtained from the single flash experiments. It should be pointed out that one cannot derive the three phases directly from the signal under repetitive excitation, since already for the two-exponential fit, the deviations between measured signal and fitting function are not well above the noise.

Reaction sequence for the electron transfer from the O_2-evolving complex to Chl a_{II}^+

With regard to an explanation for the dependence of the Chl a_{II}^+ reduction kinetics on the S-states, one has to consider the organization of the electron transfer from water to Chl a_{II}^+. There is at least one secondary donor. D, involved in electron transport from the O_2-evolving complex to Chl a_{II}^+. Flash-induced oxidation and re-reduction of D have been detected as rise and decay of an EPR signal, named signal II_{vf} (30). Recent studies, involving also optical spectroscopy, suggest that D^+ is an oxidized plastoquinol derivative [31,32]. The rise time of signal II_{vf} is not known with absolute certainty, since it has been stated recently [33] that the value of approx. 20 μs reported by Blankenship et al. [34] has to be reexamined. The decay of signal II_{vf}, has been attributed to the re-reduction of D^+ by the O_2-evolving complex [30]. From measurements in a series of four saturating flashes after dark adaptation, Babcock et al. [16] concluded that the re-reduction kinetics of D^+ depend on the S-states, prior to the flash, in the following manner:

$t_{1/2}(S_0) \lesssim 100\ \mu s$

$t_{1/2}(S_1) \lesssim 100\ \mu s$

$t_{1/2}(S_2) \approx 400\ \mu s$

and:

$t_{1/2}(S_3) \approx 1\ ms$

If D were the only secondary donor between Chl a_{II} and the O_2-evolving complex, the following kinetic scheme I should represent the electron transfer reactions on the donor side of PS II:

$$\text{Chl } a_{II}^+ \text{DS}_n \underset{k_{-1}}{\overset{k_1}{\rightleftharpoons}} \text{Chl } a_{II} \text{D}^+ \text{S}_n \underset{k_{-2}}{\overset{k_2}{\rightleftharpoons}} \text{Chl } a_{II} \text{DS}_{n+1}$$

(Scheme I)

where S_n denotes the O_2-evolving complex in the different S-states; k_i are first order rate constants which are assumed to depend on the S-states (a possible explanation for such a dependence will be discussed in the next subsection (p. 413). The equilibrium constants $K_1 = k_1/k_{-1}$ and $K_2 = k_2/k_{-2}$ should not be lower than approx. 1, since otherwise the electron transfer from the O_2-evolving complex to Chl a_{II}^+ would be very inefficient.

According to Scheme I Chl a_{II}^+ would decay biphasically down to an equilibrium level with one phase essentially determined by $k_1 + k_{-1}$ and a second phase corresponding to the decay of D^+, that is, in the below approx. 100 μs to approx. 1 ms range (see above). In contrast to this prediction, the evaluation of our experiments indicates that in state S_2 as well as in state S_3 Chl a_{II}^+ is reduced biphasically with half-times of 50 and 260 ns. Consequently, D should not be the only donor between Chl a_{II} and the O_2-evolving complex, i.e., we have to assume at least two donors, D_1 and D_2. D_2 would be the species giving rise to EPR signal II_{vf} and D_1 would be an as yet undetected donor to Chl a_{II}^+.

For the sake of simplicity, we restrict ourselves to linear electron transfer schemes and propose the following reaction sequence where, again, the rate constants k_i are assumed to depend on the S-states:

$$\text{Chl } a_{II}^+ \text{D}_1\text{D}_2\text{S}_n \underset{k_{-1}}{\overset{k_1}{\rightleftharpoons}} \text{Chl } a_{II} \text{D}_1^+ \text{D}_2\text{S}_n \underset{k_{-2}}{\overset{k_2}{\rightleftharpoons}}$$

$$\text{Chl } a_{II} \text{D}_1\text{D}_2^+ \text{S}_n \underset{k_{-3}}{\overset{k_3}{\rightleftharpoons}} \text{Chl } a_{II} \text{D}_1\text{D}_2\text{S}_{n+1}$$

(Scheme II)

Recently, Boska et al. [33] reported that in Tris-washed PS-II preparations from chloroplasts in which O_2 evolution is blocked, the rise of EPR signal II_f, which is attributed to the same species as signal II_{vf} in untreated samples, agrees with the reduction kinetics of Chl a_{II}^+. Therefore, the species giving rise to EPR signal II_f was identified as donor to Chl a_{II}^+ in Tris-washed chloroplasts. This may be in contrast to Scheme II which contains another donor, D_1, between Chl a_{II} and the species giving rise to signal II_{vf}, D_2. However, one might assume that the donor active under conditions of inhibited O_2 evolution and D_2 give rise to the same (or a similar) EPR spectrum without necessarily being the same species. In this regard, valuable information may be gained by refined measurements of rise kinetics and EPR-spectrum of signal II_{vf}.

The Chl a_{II}^+ reduction kinetics in dependence on the S-states can be calculated according to the suggested Scheme II by using the following equations, if one assumes $k_2 \gg k_{-2}$, i.e., k_{-2}, k_3 and k_{-3} do not enter into these equations:

$$\text{Chl } a_{II}^+(t,S_n) = \text{Chl } a_{II}^+(t=0)\cdot\left(a_1 e^{-r_+ t} + a_2 e^{-r_- t}\right) \quad (1)$$

with:

$$r_\pm = \tfrac{1}{2}\left(k_1 + k_{-1} + k_2 \pm \sqrt{(k_1 + k_{-1} + k_2)^2 - 4k_1k_2}\right) \quad (2)$$

$$a_1 = \frac{k_1 - r_-}{r_+ - r_-} \quad (3)$$

$$a_2 = \frac{r_+ - k_1}{r_+ - r_-} \quad (4)$$

$$t_{1/2} = \frac{\ln 2}{r} \quad (5)$$

and:

$$k_i = k_i(S_n) \quad (6)$$

Since the rate constants k_i are assumed to depend on the S-states, this is also the case for the Chl a_{II}^+ reduction kinetics given by Eqn. 1. In order to match the derived correlation between reduction kinetics and S-states (see the first subsection under Discussion, p. 409), we chose the rate constants given in Table II. We also assumed that the foreward reaction denoted by k_2 is faster in states S_0 and S_1 than in states S_2 and S_3 (for an explanation see the next subsection).

The half-life times and amplitudes of Chl a_{II}^+ reduction calculated from the rate constants in Table II, center, according to Eqns. 1–6 are listed in Table II, right, for states S_0 to S_3. A comparison between Table II, right. and the correlation proposed in the previous subsection shows quantitative agreement.

The Chl a_{II}^+ reduction kinetics in dependence on the flash number can be calculated by:

$$\text{Chl } a_{II}^+(t) = \sum_{n=0}^{3} [S_n]\,\text{Chl } a_{II}^+(t,S_n) \quad (7)$$

with:

$$\sum_{n=0}^{3} [S_n] = 1 \quad (8)$$

where $[S_n]$ denotes the population of state S_n prior to the flash.

The S-state populations prior to each flash were taken from Fig. 6c and d (circles). The results according to Eqn. 7 and Table II are depicted with broken lines in Fig. 6e and f. Fig. 6e demonstrates that the calculated amplitudes of the 23 ns phase (upper broken line) agree with the experimental results (solid line). The calculated phases with $t_{1/2} = 100$ ns (lower broken line, Fig. 6e) is too small to be resolved from the signals shown in Fig. 1. In Fig. 6f the broken line represents the sum of the calculated amplitudes of the 50 ns and the 260 ns phase. From a comparison with the experimental data we conclude:

(1) the relatively simple assumptions (Scheme II and Table II) yield an acceptable quantitative description of the experimental results;

(2) although the uncertainties of the individual amplitudes obtained by analysis of the experimental data may be in the order of $\pm 10\%$, the overall agreement with the calculated curves gives good evidence in favor of the proposed model.

Mechanism for the dependence of the Chl a_{II}^+ reduction kinetics on the S-states

An important question arising from the previous discussion is how to explain the postulated dependence of the rate constants for electron

TABLE II

RATE CONSTANTS DUE TO SCHEME II AND CALCULATED Chl a_{II}^{+} REDUCTION KINETICS (EQNS. 1–6) AT DIFFERENT S-STATES

S-state	k_1 (s^{-1})	k_{-1} (s^{-1})	k_2 (s^{-1})	$k_1/k_{-1} = K$	$t_{1/2}$ (ns)	Relative amplitude
S_0, S_1	$2.9 \cdot 10^7$	$1 \cdot 10^6$	$7 \cdot 10^6$	29	23	0.94
					100	0.06
S_2, S_3	$8.3 \cdot 10^6$	$3.8 \cdot 10^6$	$4.5 \cdot 10^6$	2.2	50	0.50
					260	0.50

transfer to Chl a_{II}^{+} on the S-states of the O_2-evolving complex. We propose that the retardation of electron transfer to Chl a_{II}^{+} in states S_2 and S_3 compared to states S_0 and S_1 is mainly caused by Coulomb attraction by a positively charged O_2-evolving complex. Electrostatic effects due to positive charges in the O_2-evolving complex have already been discussed by van Gorkom and Donze [35], with respect to experimental results on luminescence. These authors assumed that four positive charges are accumulated in the O_2-evolving complex by four subsequent turnovers of Chl a_{II} in order to evolve one oxygen molecule and four protons from water as suggested in the early scheme of Kok et al. [14].

Our results demonstrate that electron transfer to Chl a_{II}^{+} is retarded in states S_2 and S_3 compared to S_0 and S_1. Hence it would be sufficient to assume that one positive charge is formed in the O_2-evolving complex during the transition from S_1 to S_2; whereas, the transitions from S_0 to S_1 and from S_2 to S_3 do not change the net charge of the O_2-evolving complex. This means that the O_2-evolving complex in the state S_2 and S_3 is more positive by one elementary charge than in S_0 and S_1. A positively charged O_2-evolving complex in states S_2 and S_3 can be explained, if the electron release pattern (1,1,1,1) is accompanied by a proton release pattern (1,0,1,2) for the transitions ($S_0 \rightarrow S_1$, $S_1 \rightarrow S_2$, $S_2 \rightarrow S_3$, $S_3 \rightarrow S_0$). Measurement of proton release in a series of flashes after dark adaptation was controversial for some years, at present a proton release pattern (1,0,1,2) has been accepted [36–39], which is in accordance with our conclusion based on a completely different experiment.

According to Scheme II, the rate constant k_1 for electron transfer from D_1 to Chl a_{II}^{+} as well as the equilibrium constant $K = k_1/k_{-1}$ for Chl $a_{II}^{+} D_1 D_2 S \rightleftarrows$ Chl $a_{II} D_1^{+} D_2 S$ should be decreased due to a positive charge in the O_2-evolving complex in state S_2 and S_3, respectively. We assume a decrease of K from $K = 29$ in states S_0 and S_1 to $K = 2.2$ in states S_2 and S_3 (see Table II), that is, by a factor of 13. The corresponding difference of standard free-energy change, $\Delta G^0 = -\mathbf{k}T \ln K$, of the reaction can be calculated according to:

$$\Delta G_{+}^{0} - \Delta G_{0}^{0} = -\mathbf{k}T\left(\ln \frac{k_1}{k_{-1}}(S_{2,3}) - \ln \frac{k_1}{k_{-1}}(S_{0,1})\right) \qquad (9)$$

where $\mathbf{k}$ is the Boltzmann constant (the indices 0 and + denote uncharged and positively charged O_2-evolving complexes, respectively). One obtains $\Delta G_0^0 \approx -90$ meV ($\simeq -8.6$ kJ/mol) (in states S_0 and S_1) and $\Delta G_{+}^{0} \approx -20$ meV ($\simeq -1.9$ kJ/mol) (in states S_2 and S_3), respectively. Hence, the occurrence of a positive elementary charge in the O_2-evolving complex increases the change of standard free energy of the reaction by $\Delta G_{+}^{0} - \Delta G_0^0 \approx 70$ meV.

On the other hand, the change of ΔG^0 caused by the Coulomb potential of a positive elementary charge in the O_2-evolving complex can be estimated as follows. The standard free-energy change for the case of a positively charged O_2-evolving complex, ΔG_{+}^{0}, equals the value for an uncharged O_2-evolving complex, ΔG_0^0, plus an added contribution representing the change in Coulomb energy if the positive charge is transferred from Chl a_{II} to D_1 in the presence of the Coulomb potential of the positively charged O_2-evolving complex:

$$\Delta G_{+}^{0} = \Delta G_0^0 + e\left(\psi_{D_1} - \psi_{\text{Chl } a_{II}}\right) \qquad (10)$$

where e denotes the elementary charge, and ψ_{D_1} and $\psi_{\text{Chl } a_{II}}$ denote the Coulomb potential due to

TABLE III

POSSIBLE DISTANCES, $d_{\text{Chl } a_{II},S}$ AND $d_{D_1,S}$, YIELDING $\Delta G^0_+ - \Delta G^0_0 = 70$ meV ACCORDING TO EQN. 11 WITH $\epsilon_r = 4$.
For details, see text.

$d_{\text{Chl-}a_{II},S}$ (Å)	$d_{D_1,S}$ (Å)
10	8.4
15	11.6
20	14.4
25	16.8
30	18.9

the positively charged O_2-evolving complex at the centers of charge of D_1^+ and Chl a_{II}^+, respectively. Hence:

$$\Delta G^0_+ - \Delta G^0_0 = \frac{e^2}{4\pi\epsilon_0\epsilon_r}\left(\frac{1}{d_{D_1,S}} - \frac{1}{d_{\text{Chl-}a_{II},S}}\right) \quad (11)$$

ϵ_0, dielectric constant of the vacuum; ϵ_r, relative dielectric constant, $d_{D_1,S}$, distance between the positive charge on D_1 and the positive charge on the O_2-evolving complex in states S_2 and S_3, $d_{\text{Chl } a_{II},S}$, distance between the positive charge on Chl a_{II} and the positive charge on the O_2-evolving complex in states S_2 and S_3. This is only a rough approximation, since we have assumed point charges and have neglected spatial variations of the dielectric constant and changes of entropy due to conformational changes caused by the formation of the positive charge.

Dielectric constants in the order of $\epsilon_r \approx 4$ are typical for biological membranes. Table III demonstrates that $\Delta G^0_+ - \Delta G^0_0 = 70$ meV and, hence, a decrease of the equilibrium constant K by a factor of 13 can be realized assuming plausible distances, resulting in $d_{\text{Chl } a_{II},D_1} \geq 5.6$ Å, e.g., $d_{D_1,S} = 14.4$ Å and $d_{\text{Chl } a_{II},S} = 20$ Å.

Qualitatively, the positive charge in the O_2-evolving complex may also explain the decrease of rate constant k_1 for electron transfer from D_1 to Chl a_{II}^+ by a facor of about 3 (see Table II). The decrease of k_1 can be described, e.g., within the framework of the Marcus theory for electron-transfer reactions. The Marcus theory predicts a decrease of the rate of the foreward reaction if ΔG^0 is increased due to an electric field, except for 'highly exothermic' reactions [40]. Thus, in our case, where ΔG^0 in only slightly negative, the increase of ΔG^0 due to a positive elementary charge in the O_2-evolving complex qualitatively explains the decrease of rate constant k_1. Correspondingly, a positive charge in the O_2-evolving complex should also decrease k_2, as assumed in the previous subsection (p. 411).

These estimations demonstrate that electrostatic effects due to a positively charged O_2-evolving complex may well explain the retardation of electron transfer to Chl a_{II}^+ in states S_2 and S_3 compared to states S_0 and S_1.

Acknowledgements

We thank Dr. H.-E. Åkerlund for suggesting the procedure for preparation of the subchloroplasts and Dr. G.H. Schatz for valuable discussions. This work was supported by grants from the Deutsche Forschungsgemeinschaft/Sonderforschungsbereich 9, Teilprojekt C9.

References

1 Döring, G., Stiehl, H.H. and Witt, H.T. (1967) Z. Naturforsch. 22b, 639–644
2 Döring, G., Renger, G., Vater, J. and Witt, H.T. (1969) Z. Naturforsch. 24b, 1139–1143
3 Stiehl, H.H. and Witt, H.T. (1968) Z. Naturforsch. 23b, 220–224
4 Stiehl, H.H. and Witt, H.T. (1969) Z. Naturforsch. 24b, 1588–1598
5 Haveman, J. and Mathis, P. (1976) Biochim. Biophys. Acta 440, 346–355
6 Van Gorkom, H.J., Pulles, M.P.J. and Wessels, J.S.C. (1975) Biochim. Biophys. Acta 408, 331–339
7 Schlodder, E., Brettel, K., Schatz, G.H. and Witt, H.T. (1984) Biochim. Biophys. Acta 765, 178–185
8 Van Best, J.A. and Mathis, P. (1978) Biochim. Biophys. Acta 505, 178–188
9 Mauzerall, D. (1972) Proc. Natl. Acad. Sci. USA 69, 1358–1362
10 Sonneveld, A., Rademaker, H. and Duysens, L.N.M. (1979) Biochim. Biophys. Acta 548, 536–551
11 Deprez, J., Dobek, A., Geacintov, N.E., Paillotin, G. and Breton, J. (1983) Biochim. Biophys. Acta 725, 444–454
12 Brettel, K. and Witt, H.T. (1983) Photobiochem. Photobiophys. 6, 253–260
13 Joliot, P., Barbieri, G. and Chabaud, R. (1969) Photochem. Photobiol. 10, 309–329
14 Kok, B., Forbush, B. and McGloin, M. (1970) Photochem. Photobiol. 11, 457–475
15 Forbush, B., Kok, B. and McGloin, P. (1971) Photochem. Photobiol. 14, 307–321

16 Babcock, G.T., Blankenship, R.E. and Sauer, K. (1976) FEBS Lett. 61, 286–289
17 Zankel, K. (1971) Biochim. Biophys. Acta 245, 373–385
18 Delosme, R. (1972) in Proceedings of the 2nd International Congress on Photosynthesis (Forti, G., Avron, M. and Melandri, A., eds.), pp. 187–195, Dr. W. Junk N.V. Publishers, The Hague
20 Gläser, M., Wolff, Ch. and Renger, G. (1976) Z. Naturforsch. 31c, 712–721
20 Åkerlund, H.-E., Jansson, C. and Andersson, B. (1982) Biochim. Biophys. Acta 681, 1–10
21 Schatz, G.H. and Witt, H.T. (1984) Photobiochem. Photobiophys. 7, 1–14
22 Bevington, P.R. (1969) Data Reduction and Error Analysis for the Physical Sciences, McGraw-Hill Book Company, New York
23 Mathis, P. and Setif, P. (1981) Isr. J. chem. 21, 316–320
24 Gläser, M., Wolff, Ch., Buchwald, H.E. and Witt, H.T. (1974) FEBS Lett. 42, 81–85
25 Renger, G., Eckert, H.-J. and Buchwald, H.E. (1978) FEBS Lett. 90. 10–14
26 Conjeaud, H., Mathis, P. and Paillotin, G. (1979) Biochim. Biophys. Acta 546, 280–291
27 Bouges-Bocquet, B. (1973) Biochim. Biophys. Acta 292, 772–785
28 Jursinic, P. (1981) Biochim. Biophys. Acta 635, 38–52
29 Renger, G., Bouges-Bocquet, B. and Delosme, R. (1973) Biochim. Biophys. Acta 292, 796–807
30 Blankenship, R.E., Babcock, G.T., Warden, J.T. and Sauer, K. (1975) FEBS Lett. 51, 287–293
31 Babcock, G.T., Buttner, W.J., Ghanotakis, D.F., O'Malley, P.J., Yerkes, C.T. and Yocum, C.F. (1984) in Advances in Photosyntheis Research (Sybesma, C., ed.), Vol. I, pp. 243–252, Martinus Nijhoff/Dr. W. Junk Publishers, The Hague
32 Dekker, J.P., Brok, M. and Van Gorkom, H.J. (1984) in Advances in Photosynthesis Research (Sybesma, C., ed.), Vol. I, pp. 171–174, Martinus Nijhoff/Dr. W. Junk Publishers, The Hague
33 Boska, M., Sauer, K., Buttner, W. and Babcock, G.T. (1983) Biochim. Biophys. Acta 722, 327–330
34 Blankenship, R.E., McGuire, A. and Sauer, K. (1977) Biochim. Biophys. Acta 459, 617–619
35 Van Gorkom, H.J. and Donze, M. (1973) Photochem. Photobiol. 17, 333–342
36 Fowler, C.F. (1977) Biochim. Biophys. Acta 462, 414–421
37 Saphon, S. and Crofts, A.R. (1977) Z. Naturforsch. 32c, 617–626
38 Velthuys, B.R. (1980) FEBS Lett. 115, 167–70
39 Förster, V., Hong, Y.-Q. and Junge, W. (1981) Biochim. Biophys. Acta 638, 141–152
40 Marcus, R.A. (1979) in Light-induced Charge Separation in Biology and Chemistry (Gerischer, H. and Katz, J.J., eds.), pp. 15–43, Verlag Chemie, Weinheim